

# Prediction of Wearing of Cutting Tools Using Real Time Machining Parameters and Temperature Using Rayleigh-Ham Method

Jean Nyatte Nyatte<sup>1,2</sup>, Fabrice Alban Epee<sup>1</sup>, Wilba Christophe Kikmo<sup>1</sup>, Samuel Batambock<sup>1</sup>, Claude Valéry Ngayihi Abbe<sup>1\*</sup>, Robert Nzengwa<sup>1</sup>

<sup>1</sup>E3M Laboratory, National Higher Polytechnic School Douala, University of Douala, Douala, Cameroon

<sup>2</sup>Institut Universitaire de Technologie (IUT-BOIS), University of Yaoundé I, Mbalmayo, Cameroon

Email: \*ngayihiclaude@yahoo.fr

**How to cite this paper:** Nyatte Nyatte, J., Epee, F.A., Kikmo, W.C., Batambock, S., Ngayihi Abbe, C.V. and Nzengwa, R. (2023) Prediction of Wearing of Cutting Tools Using Real Time Machining Parameters and Temperature Using Rayleigh-Ham Method. *Modern Mechanical Engineering*, **13**, 35-54. <https://doi.org/10.4236/mme.2023.132003>

**Received:** January 11, 2023

**Accepted:** May 28, 2023

**Published:** May 31, 2023

Copyright © 2023 by author(s) and Scientific Research Publishing Inc.

This work is licensed under the Creative Commons Attribution International License (CC BY 4.0).

<http://creativecommons.org/licenses/by/4.0/>



Open Access

## Abstract

Wear of cutting tools is a big concern for industrial manufacturers, because of their acquisition cost as well as the impact on the production lines when they are unavailable. Law of wear is very important in determining cutting tools lifespan, but most of the existing models don't take into account the cutting temperature. In this work, the theoretical and experimental results of a dynamic study of metal machining against cutting temperature of a treated steel of grade S235JR with a high-speed steel tool are provided. This study is based on the analysis of two complementary approaches, an experimental approach with the measurement of the temperature and on the other hand, an approach using modeling. Based on unifactorial and multifactorial tests (speed of cut, feed, and depth of cut), this study allowed the highlighting of the influence of the cutting temperature on the machining time. To achieve this objective, two specific approaches have been selected. The first was to measure the temperature of the cutting tool and the second was to determine the wear law using Rayleigh-Ham dimensional analysis method. This study permitted the determination of a law that integrates the cutting temperature in the calculations of the lifespan of the tools during machining.

## Keywords

Machining, Cutting Temperature, Modeling, Wear, Cutting Tool

## 1. Introduction

Conventional machining processes by material removal, such as turning, drilling and milling, etc., subject the tool to plastic deformation when cutting metals. Wear is considered to be one of the primary phenomena affecting cutting tools

during machining operations. Knowledge of the evolution of wear over time allows operators working on machine tools to maximize the performance of cutting tools and improve the quality of the surfaces of machined parts [1]. However, knowing this parameter is not the only clue to deciding whether to stop or continue machining. Other parameters influence the machining process, such as cutting conditions, tool material, workpiece material, cutting temperature, cutting force as well as machine tools and the work environment. It is known in advance that worn cutting tools compromise the surface finish of parts [2] [3] [4] [5]. It is to overcome the consequences of the wear of the cutting tools, which is imperative to develop modeling, evaluation and monitoring systems of the cutting tools for the machine tools [6] [7] [8]. All these systems must very quickly alert the machine tool operator of the state of deterioration and damage to the cutting edge of the cutting tool. Several systems exist and are based on the development of mathematical and computer models, automatic monitoring and finally the identification of tool wear [9] [10] [11] [12] [13]. **Figure 1** describes the temperature distribution around the cutting zone [14]. Many researchers [15] [16] [17] believe that monitoring the cutting temperature can provide valuable information on the importance of the thermal effects associated with the cut, particularly with regard to the holding of the tool.

Machining is practiced either as lubricated or dry. Dry machining saves lubricant and tool life  $T$  (min) can also be shortened.

However, the temperature in the contact zone of the tool and the chip is higher than in machining using the lubricant. Recent studies support that the chips evacuate at least eighty-five percent of the heat generated by the cut [18]. Research shows that the mode of chip evacuation [19] [20] [21] is important and limits their influence in the cutting zone, in order to facilitate their recovery. The prediction of the geometry of the formed chip depends on the influence of the geometry of the active part of the tool on the plastic deformation [22]. It is essential to evacuate the chips because they contain 85% of the heat released in the cutting zone [23]. Lubrication is a set of techniques that reduce friction and wear between the workpiece and the cutting tool. It makes it possible to evacuate part of the thermal energy generated by friction, as well as to avoid corrosion [24].

In order to measure the cutting temperature, several techniques exist, including the tool-workpiece thermocouple, the inserted thermocouple, spectral radiation thermography and the recently proposed thin-film thermal sensor [25] [26] [27] [28]. However, these techniques cannot provide any information on the chipping, breakage and catastrophic failure of the cutting tools, nor on their service life [8] [29] [30]. The cutting forces are at the origin of the plastic deformation of the machined material in the various shearing zones, causing the formation of the chip and consequently contributing to the wear of the cutting tool. They can be decomposed as shown in **Figure 2** [31] [32] [33] [34].

From the above literature it is clear that in order to effectively monitor the wear of cutting tools, which influences its lifespan, and the surface condition of parts during machining operations, we should determine the influence of the

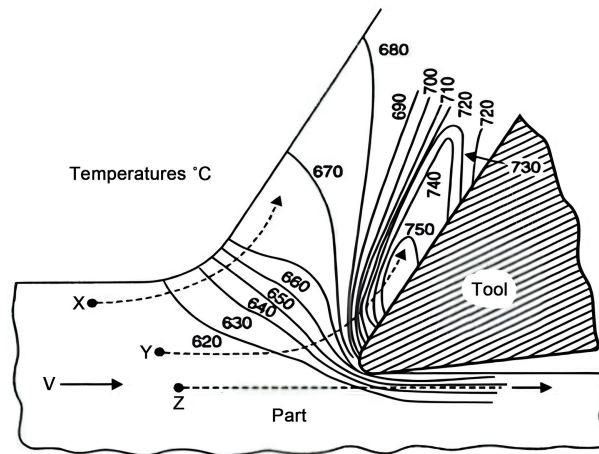


**Figure 1.** Distribution of temperatures in orthogonal section [14].

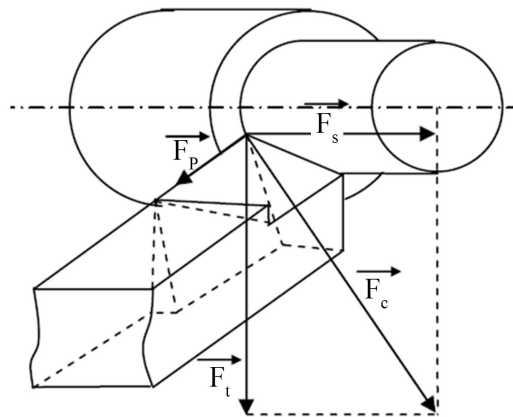


**Figure 2.** Decomposition of cutting forces.  $F_t$ . Tangential force;  $F_a$ : Effort in advance;  $F_p$ . Force of repulsion (negligible in the case of an orthogonal cut);  $F_c$ . Cutting force. J. Vergnas [11].

cutting temperature, the speed of cut, the density of the material to be machined, and the thermal conductivity. In doing so a reliable wear law model can be determined. This article aims to present the influence of the cutting temperature on the lifespan of cutting tools and to propose a new mathematical model of the wear law.

## 2. Materials and Methods

In this study, we implement a temporary device to measure the temperature at the tool tip during the turning operation on a digital display lathe. A block diagram of the experimental device is presented in **Figure 3**. The temperature measurement device is an STC-1000 (Sound Transfer Class) measurement sensor. The high speed steel knife tool was used during this study. A 4 mm diameter cable connects the sensor to the probe so as to touch the active part of the tool. In this arrangement, the temperature detected on the active part of the tool will be displayed on the sensor. The tool is fixed on the tool holder and the workpiece is fixed on the four-jaw chuck. The reading of the temperature values dis-

played on the SCT-1000 sensor is carried out for different machining conditions when varying the cutting parameters such as the feed rate, the depth of cut, the rotational speed and speed of cut.

### 2.1. Digital Display Tower

Lathe is the name of the machine tool used for the turning process. Turning is a metalworking process in which the workpiece is rotated and a single point cutting tool made of hard material is brought to the surface of the workpiece resulting in the removal of the excess material in the form of chips.

### 2.2. Work Piece

A treated mild steel specimen of grade S235JR of cylindrical shape is chosen as the workpiece for the experiment. Mild steel is chosen because it has wide application in the manufacture of worms, gears, machine parts, tool die set components, tool holders, etc. and also, because it is available at low cost.

### 2.3. Cutting Tool

In this project, we measure the temperature on the cutting tool during the turning operation. The tool used for this experiment is a straight knife tool with a high-speed steel tip.

### 2.4. SCT-1000 Temperature Measurement Sensor

The SCT-1000 sensor is used for temperature measurement in this experiment. The temperature measurement range of this equipment is  $-30^{\circ}\text{C}$  up to  $1200$  degrees Celsius and covers emissivities from  $0.10$  to  $1.00$  from  $-200$  to  $1250$  degrees Celsius. The SCT-1000 sensor only measures the corresponding temperature. The measured value is displayed and is read, stored, processed and evaluated.

### 2.5. Block Diagram

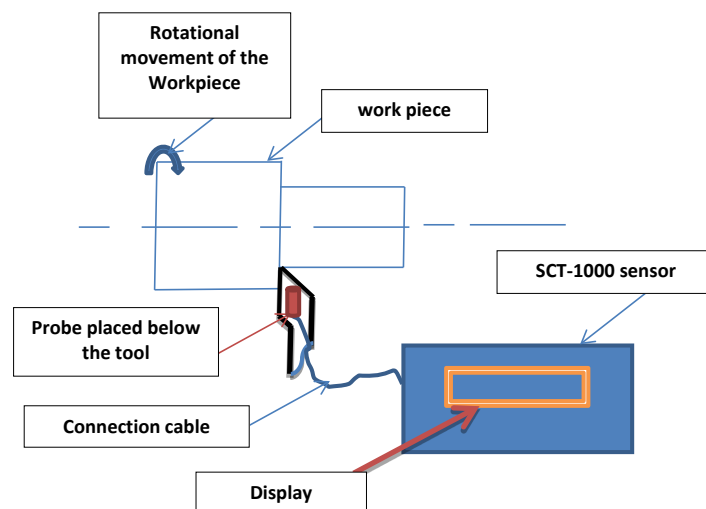


**Figure 3.** Diagram of the experimental device.

## 2.6. Procedure

The diameter of the sensor probe placed below the active part of the tool is measured then the cable that connects the probe to the sensor is measured. The knife tool is fixed on the tool holder while the workpiece is centered on one end and securely mounted on the four-jaw chuck of the digital display lathe. One end of the cable is connected to the probe on the tool side, and the other end is connected to the SCT-1000 sensor. The parameters taken into account are the feed rate, the depth of cut and the rotational speed in rpm and the feed rate.

Calculations have been made to find the values of the rotational speeds and the forward speed while the depth of pass varies and is regulated. Temperature values were determined from display readings; the displayed values of the temperature measurement sensor are recorded and stored for different measurement values. Cutting conditions are presented in **Table 1**. The same procedure is repeated for different temperature measurement values. After each turning operation, a time of seven minutes was allowed for the tool to cool down to the initial state of atmospheric temperature. Graphs have been plotted to obtain the relationship between temperature and the various parameters.

## 2.7. Design of the Mathematical Model

### 2.7.1. Dimensional Analysis of the Model by the Rayleigh-Ham Method

The dimensional analysis by Rayleigh-Ham method will provide us the unit or association of units in which the result will be expressed. This analysis will allow us to check on the validity of the proposed formula. We consider the machining time as a function of the temperature  $D = (T/\theta) = F(V, \rho, Q, \lambda)$ . **Table 2** below presents the dimension data.

**Table 1.** Values of cutting conditions.

	Feedrate (F) (mm/min)	Speed of cut (Vc) (m/min)	Depth of pass (ap) (mm)
Slow	0.25	2.35	0.5
Medium	4	36.6	0.7
High	13.3	125.2	0.8

**Table 2.** Data of basic dimensions.

	$\alpha$	$\beta$	$\gamma$	$\delta$	$\epsilon$
	$V$	$\rho$	$Q$	$D$	$\lambda$
Length	1	-3	3	0	0
Mass	0	1	0	0	0
Time	-1	0	-1	1	0
°K	0	0	0	0	1

**2.7.2. Calculation of Parameters ( $\alpha, \beta, \gamma, \delta, \varepsilon$ )**

$$\begin{aligned} \alpha - 3\beta + 3\gamma + \varepsilon &= 0 \\ \beta + \varepsilon &= 0 \\ -\alpha - \gamma + \delta - 3\varepsilon &= 0 \\ -\delta - \varepsilon &= 0 \end{aligned} \tag{2.1}$$

After solving this system of equations, we have:

$$\begin{cases} \alpha = -4\varepsilon \\ \beta = -\varepsilon \\ \gamma = 0 \\ \delta = -\varepsilon \\ \varepsilon = 1 \end{cases}$$

We know that:

$$V^\alpha \times \rho^\beta \times Q^\gamma \times D^\delta \times \lambda^\varepsilon = Cte$$

By replacing these parameters by their values, we obtain:

$$V^{-4} \times \rho^{-1} \times Q^0 \times D^{-1} \times \lambda^1 = Cte \tag{2.2}$$

Knowing that:

$$D = \frac{T}{\theta}$$

We obtain:

$$\frac{\lambda}{V^4 \rho D} = \frac{T}{\theta} \tag{2.3}$$

Replacing by its value  $\frac{T}{\theta}$

$$T = \frac{\theta \lambda}{V^4 \rho} \tag{2.4}$$

**Verification of units:**

$D/K$ : Duration according to temperature (S/K).

$V$ : speed in (m/s).

$\rho$ : density of the material (Kg/m<sup>3</sup>).

$Q$ : Chip volume (m<sup>3</sup>/s).

$\lambda$ : Thermal conductivity (Kg·m/(S<sup>3</sup>·K)).

We have:

$$S = \frac{K \cdot Kg \cdot m \cdot S^4 \cdot m^3}{S^3 \cdot Km^4 \cdot Kg} \tag{2.5}$$

**After simplifying similar terms, we find that:**

$$S = S \tag{2.6}$$

The units being verified, we can consider that the model is homogeneous and therefore the dimensional analysis is validated.

**3. Results and Discussions**

The experiment of measuring the cutting temperature during machining was

successfully carried out using an SCT-1000 sensor. During these tests, and for each specimen, we keep, for each turning operation, the selected rotational speed constant to vary the depth of passes. The temperature is the parameter followed during this experimental work and the values of the cutting temperatures were measured by the sensor at three different depths of cut. The experiment is repeated at three different feed, cutting and rotation speeds and the values obtained from one of the tables are presented below. During this experiment, we drew up five tables, three for a cutting length  $L_c = 35$  mm and two tables for a cutting length  $L_c = 25$  mm.

### 3.1. Graphic Representation of Curves

The data of the different tables were used to draw the curves below:

- The temperature curve as a function of the depth of cut ( $a_p$  in mm);
- The curve of the temperature according to the rotational speed ( $N$  in rpm);
- The temperature curve as a function of the speed of cut ( $V_c$  in m/min);
- The temperature curve as a function of the feed rate ( $F$  in mm/min).

**Table 3** and **Table 4** present values of speed of cuts ( $V_c$ ), feedrates ( $F$ ), depths of cut ( $a_p$ ) and temperatures ( $^{\circ}C$ ) for machining operations for different series, and made it possible to plot the various curves.

**Table 3.** Values of speed of cuts ( $V_c$ ), feedrates ( $F$ ), depths of cut ( $a_p$ ) and temperatures ( $^{\circ}C$ ) for machining operations in the 1-2-3 series for  $L_c = 35$  mm.

$V_c$	$F$	$A_p$	$^{\circ}C$
2.35	0.25	0.8	27
2.29	0.25	1.5	26.7
2.23	0.25	2	26.5
3.29	0.35	0.8	30
3.2	0.35	0.7	29.7
3.13	0.35	0.5	27.4
5.18	0.55	0.8	32.1
5	0.55	0.7	31.5
4.92	0.55	0.5	31
8.0	0.85	0.8	33.6
7.79	0.85	0.7	32.7
7.60	0.85	0.5	31.5
11.3	1.2	0.8	34.7
11	1.2	1.5	33.3
10.7	1.2	2	32.9
17.4	1.85	0.8	35
16.9	1.85	1.5	34.7
16.5	1.85	2	33.8
25.9	2.75	0.8	38.2
25.2	2.75	1.5	37.3
24.6	2.75	2	36.6

**Continued**

37.6	4	0.8	39.9
36.6	4	1.5	38.2
35.7	4	2	37.7
37.6	4	0.8	36.6
36.6	4	1.5	35.9
35.1	4	2	35.5
56.9	6.05	0.8	39.3
55.4	6.05	1.5	34.7
54.1	6.05	2	39.3
85.7	9.1	0.8	40.1
83.4	9.1	1.5	38.4
81.4	9.1	2	37.4
125.2	13.3	0.8	42.9
121.9	13.3	1.5	41.4
119	13.3	2	38.7

**Table 4.** Values of speed of cuts (Vc), feedrates (F), depths of cut (ap) and temperatures ( $\theta^{\circ}C$ ) machining series 4 and 5 for Lc = 25 mm.

Vc	F	Ap	$\theta^{\circ}C$
3.29	0.35	0.8	27
3.20	0.35	1.5	26.7
3.13	0.35	2	26.5
5.18	0.55	0.8	30
5	0.55	1.5	29.6
4.92	0.55	2	27.1
8	0.85	0.8	32.1
7.79	0.85	1.5	31.5
7.60	0.85	2	31
11.3	1.2	0.8	33.6
11	1.2	1.5	32.7
10.7	1.2	2	31.5
17.4	1.85	0.8	34.9
16.9	1.85	1.5	34.7
16.5	1.85	2	33.8
25.9	2.75	0.8	38
25.2	2.75	1.5	37
24.6	2.75	2	36
37.6	4	0.8	39
36.6	4	1.5	38.1
35.7	4	2	37.6
56.9	60.5	0.8	39.3
55.4	60.5	1.5	38
54.1	60.5	2	37.1

Figures 4-8 present comparative curves of temperature as a function of the depth of cut with a variable rotation speed (N) for different series.

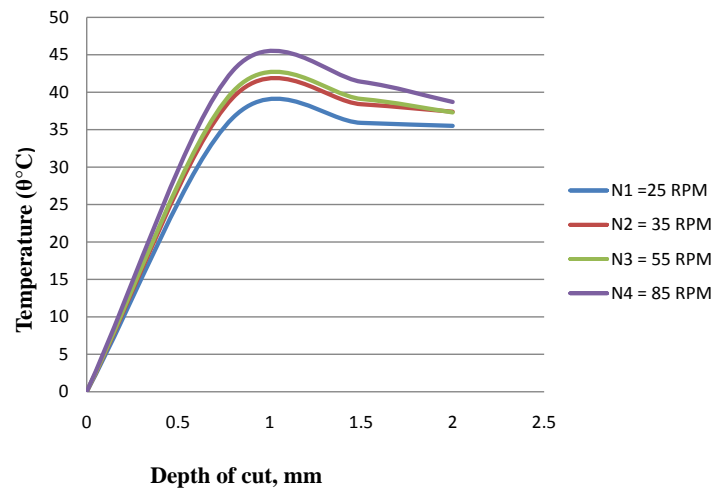


Figure 4. Curves of temperature as a function of the depth of cut with a variable rotation speed (N in RPM). Machining series 1,  $L_c = 35$  mm.

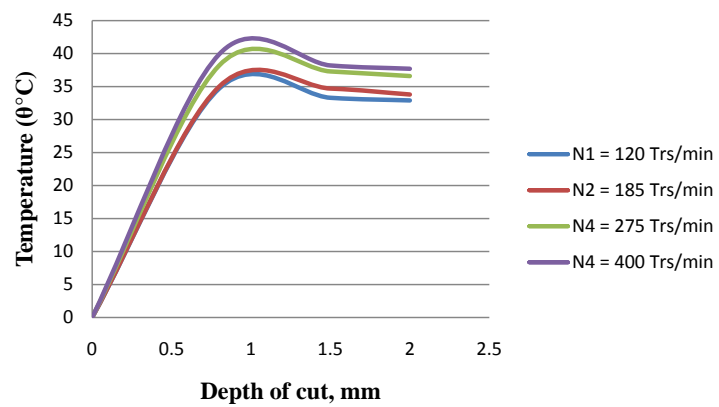


Figure 5. Curves of temperature as a function of the depth of cut with a variable rotation speed (N in RPM). Machining series 2,  $L_c = 35$  mm.

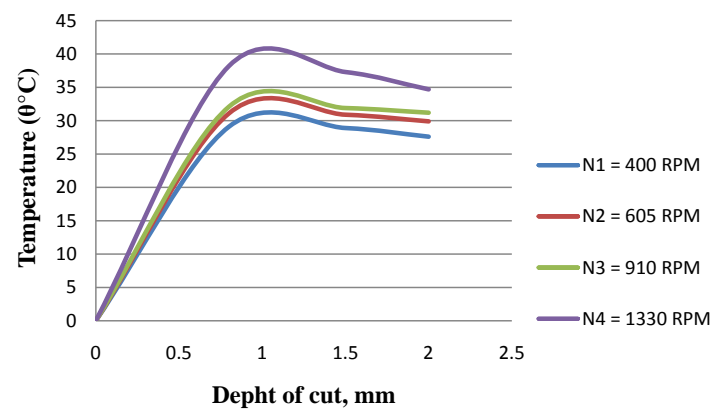
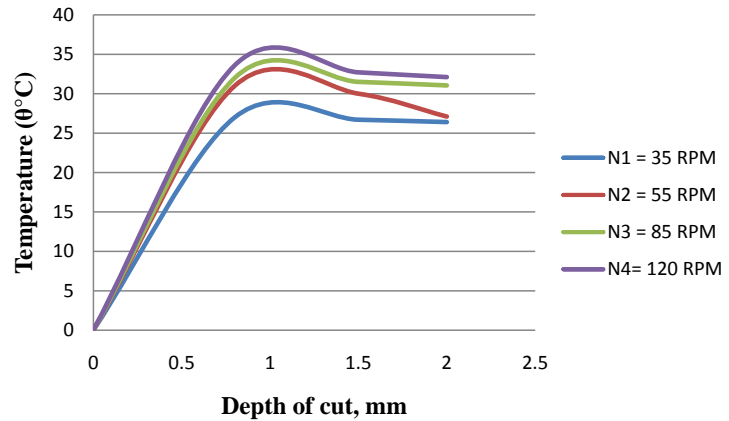
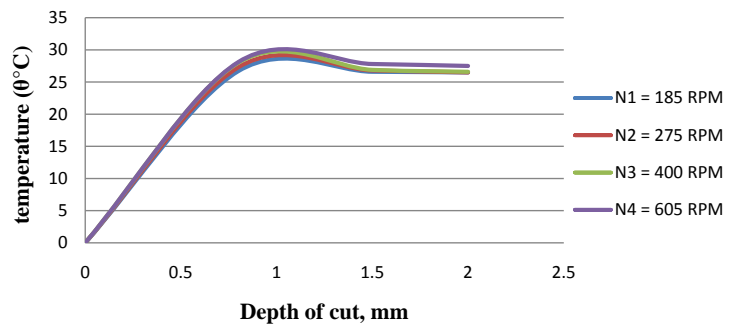


Figure 6. Curves of temperature as a function of the depth of cut with a variable rotation speed (N in RPM). Machining series 3,  $L_c = 35$  mm.



**Figure 7.** Curves of temperature as a function of the depth of cut with a variable rotation speed (N in RPM). Machining series 4,  $L_c = 25$  mm.



**Figure 8.** Curves of temperature as a function of the depth of cut with a variable rotation speed (N in RPM). Machining series 5,  $L_c = 35$  mm.

### 3.2. Curves of Temperature According to the Depth of Cut

The data in **Table 2** resulting from the machining of twelve specimens made it possible to draw twelve curves showing the variation in temperature ( $\theta^\circ C$ ) as a function of the depth of cut (ap in mm); and for a cutting length  $L_c = 35$  mm.

Below, the machining data are from machining series 4 and 5.

The data in **Table 3** resulting from the machining of eight specimens made it possible to draw eight curves showing the variation in temperature ( $\theta^\circ C$ ) as a function of the depth of cut (ap in mm); and for a cutting length  $L_c = 25$  mm.

### 3.3. Discussion on the Curves of Temperature According to the Depth of Cut

By observing all the curves drawn from the data resulting from the various machining operations and on all the series of machining operations carried out (1-2-3-4-5), for the cutting lengths  $L_c = 35$  mm (series 1-2-3) and  $L_c = 25$  mm (series 4-5), we observe a similarity in the appearance of the curves and a correlation. When the depth of cut increases (start of machining from 0 to 0.8 mm), the temperature tends to increase. When the depth of cut is low (between 0.8 - 1.5 mm), the temperature drops and tends to stabilize for a depth of cut of between (1.5 - 2 mm).

### 3.4. Temperature Curves as a Function of Rotation Speed (N in rpm)

The values taken from **Table 2** and **Table 3** made it possible to plot the curves describing the variation of temperature as a function of the rotational speed (**Figures 9-13**), for length of  $L_c = 35$  mm and  $L_c = 25$  mm.

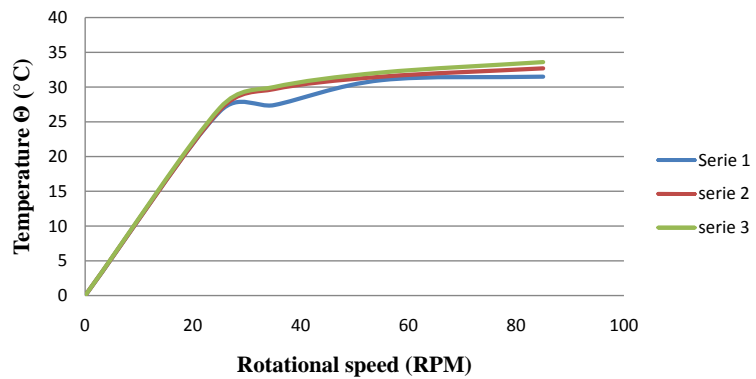


**Figure 9.** The curves of temperature according to the rotational speed with an advance  $f = 0.01$  mm. Machining series 1,  $L_c = 35$  mm.

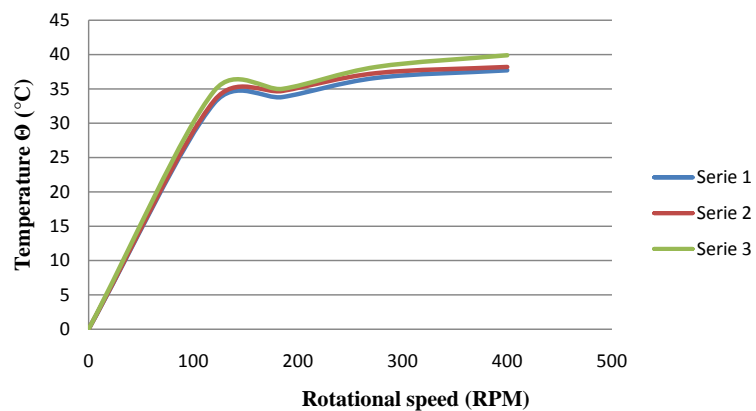


**Figure 10.** The curves of temperature according to the rotational speed with an advance  $f = 0.01$  mm. Machining series 2,  $L_c = 35$  mm.

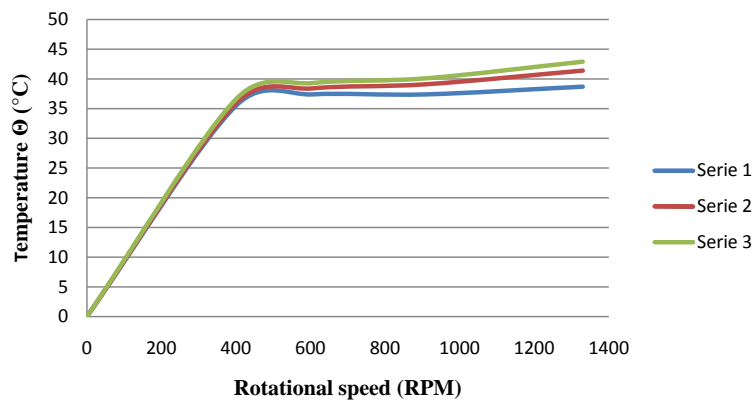


**Figure 11.** The curves of temperature according to the rotational speed with an advance  $f = 0.01$  mm. Machining series 3,  $L_c = 35$  mm.

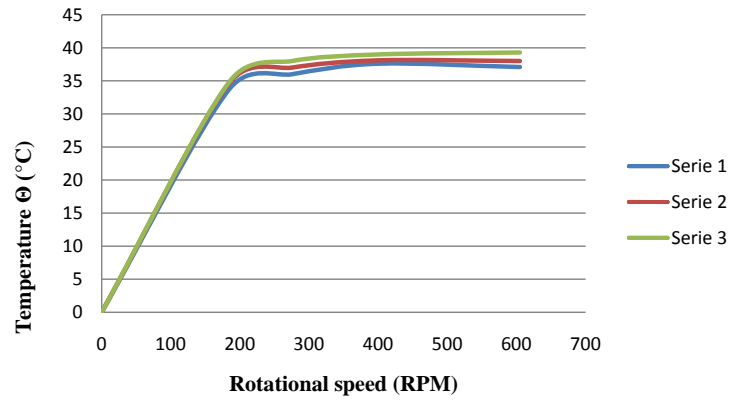


**Figure 12.** The curves of temperature according to the rotational speed with an advance  $f = 0.01$  mm. Machining series 4,  $L_c = 25$  mm.

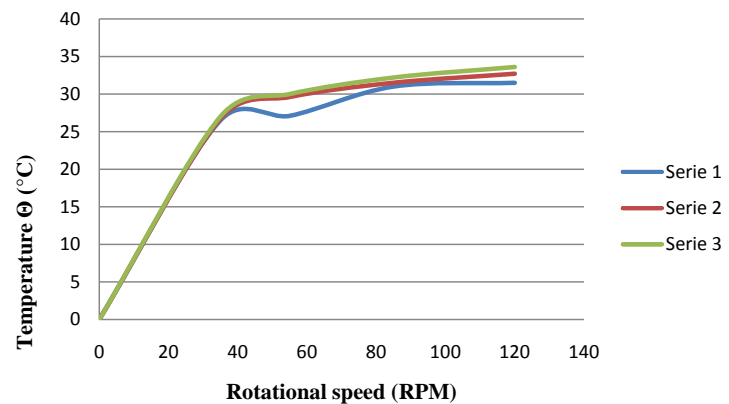


**Figure 13.** The curves of temperature according to the rotational speed with an advance  $f = 0.01$  mm. Machining series 5,  $L_c = 25$  mm.

### 3.5. Discussion on Temperature Curves as a Function of Rotational Speed

The curves above (Figures 9-13) drawn from the data taken from the (Table 2 and Table 3), for different cutting lengths ( $L_c = 25$  mm and  $L_c = 35$  mm) show a similarity. We find that, when we vary the rotational speed ( $N$ ), the temperature increases remarkably. This increase in heat can accelerate the deterioration of the cutting edge of the cutting tool.

### 3.6. Curves of Temperature ( $\theta^{\circ}\text{C}$ ) According to the Speed of Cut ( $V_c$ )

The values taken from Table 2 and Table 3 made it possible to plot the curves of temperature as a function of the speed of cut with a feed  $f = 0.01$  mm (Figures 14-18), for a length of  $L_c = 35$  mm and  $L_c = 25$  mm

### 3.7. Discussion on Temperature Curves as a Function of Speed of Cut

The curves above (Figures 14-18) drawn from the data taken from (Table 2 and

**Table 3**), for different cutting lengths ( $L_c = 25$  mm and  $L_c = 35$  mm) show a similarity. We find that, when the speed of cut is varied, the temperature increases remarkably. This increase in heat can accelerate the deterioration of the cutting edge of the cutting tool.

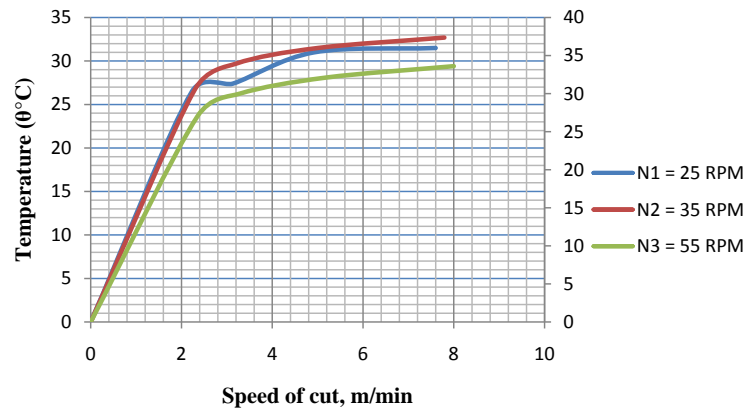


**Figure 14.** Curves of temperature as a function of the speed of cut with a feed  $f = 0.01$  mm,  $N$  variable. Machining series 1,  $L_c = 35$  mm.

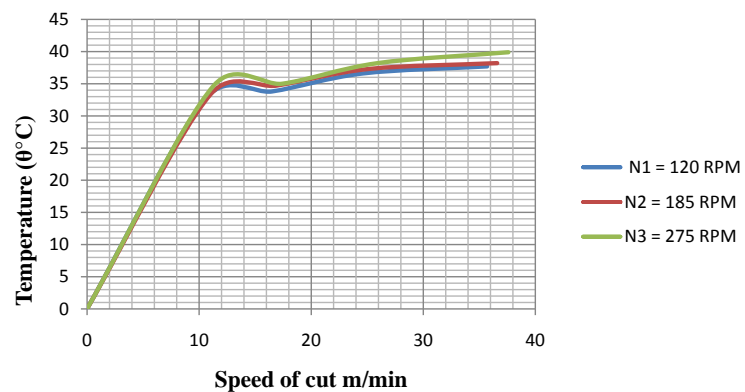


**Figure 15.** Curves of temperature as a function of the speed of cut with a feed  $f = 0.01$  mm,  $N$  variable. Machining series 2,  $L_c = 35$  mm.

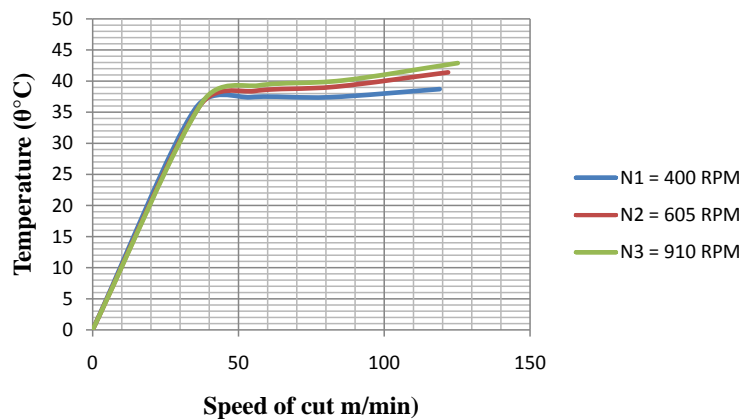


**Figure 16.** Curves of temperature as a function of the speed of cut with a feed  $f = 0.01$  mm,  $N$  variable. Machining series 3,  $L_c = 35$  mm.

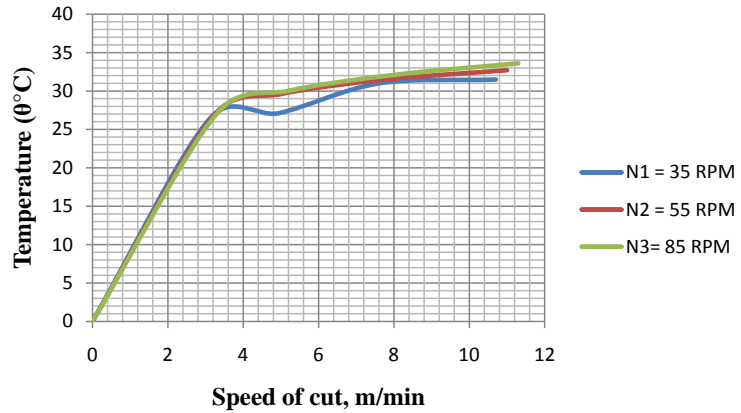


**Figure 17.** Curves of temperature as a function of speed of cut with a variable N. Machining series 4,  $L_c = 25$  mm.

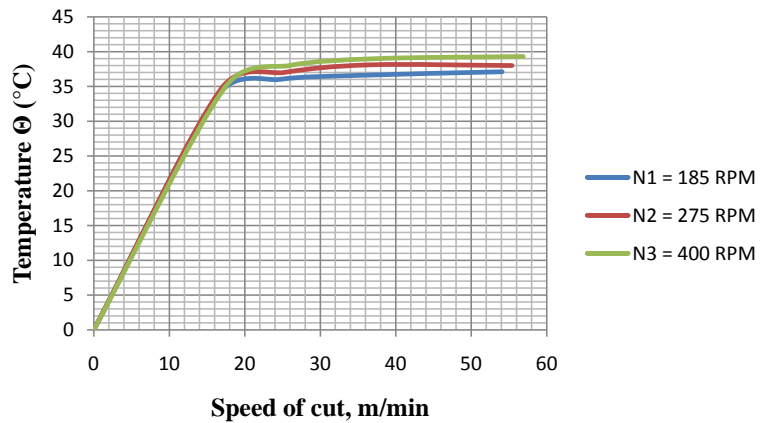


**Figure 18.** Curves of temperature as a function of speed of cut with a variable N. Machining series 5,  $L_c = 25$  mm.

### 3.8. Curves of the Temperature ( $\theta^\circ\text{C}$ ) According to the Feedrate (F)

The values taken from **Table 2** and **Table 3** made it possible to draw the curves below, for a length of  $L_c = 35$  mm.

The data in **Table 3** resulting from the machining of eight specimens made it possible to draw eight curves showing the variation in temperature ( $\theta^\circ\text{C}$ ) as a function of the feedrate (F in mm/min); and for a cutting length  $L_c = 25$  mm.

### 3.9. Discussion on Temperature Curves as a Function of Feed Rate

The curves above (**Figures 19-23**) plotted using data from (**Table 2** and **Table 3**), for different cutting lengths ( $L_c = 25$  mm and  $L_c = 35$  mm). From the analysis of the graphs above, it appears that the increase in the feed rate generates an increase in friction and deformations, which raises the temperature in the different cutting zones of the machining series 1-2 -3-4 and 5. During these operations, the maximum heat is evacuated by the chip, this prevents the phenomena of thermal expansion of the part to be machined.

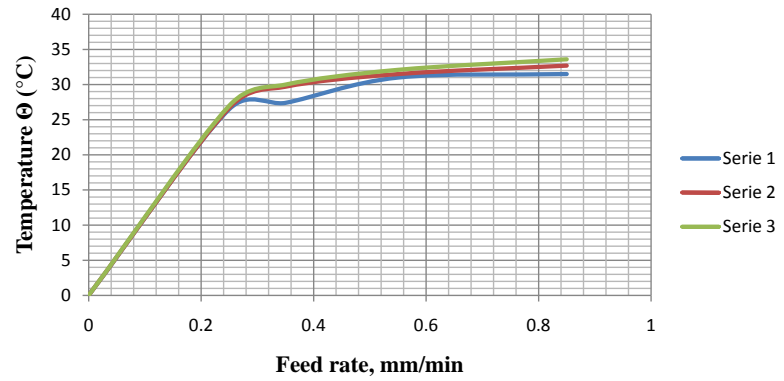


**Figure 19.** Curves of temperature as a function of the feedrate. Machining series 1,  $L_c = 35$  mm.

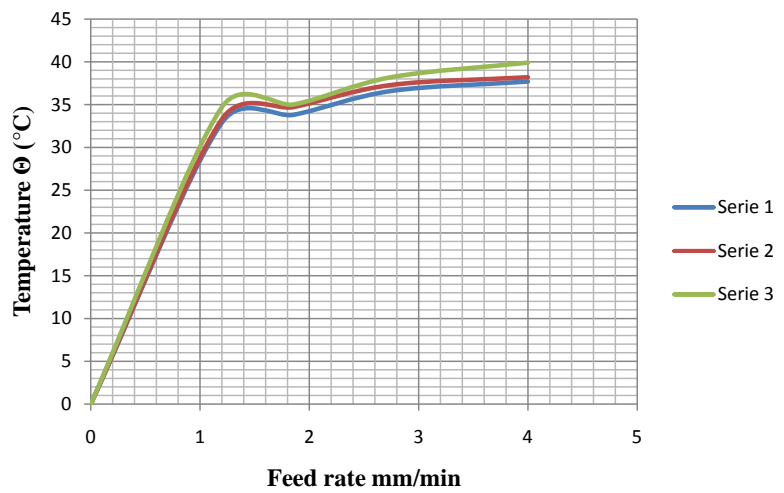


**Figure 20.** Curves of temperature as a function of the feedrate. Machining series 1,  $L_c = 35$  mm.

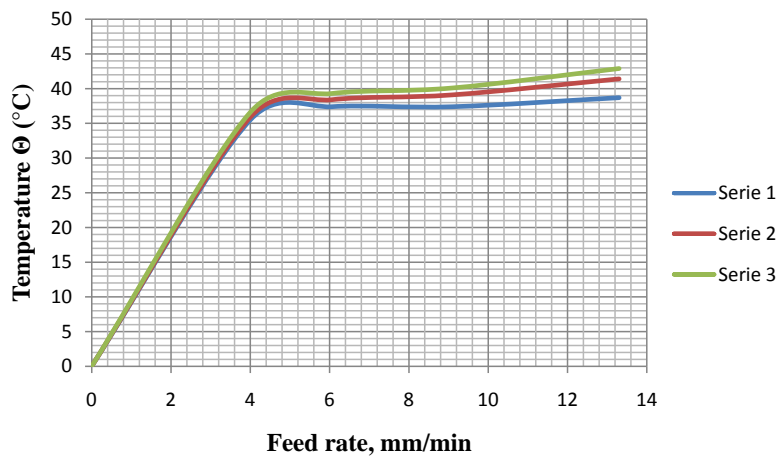


**Figure 21.** Curves of temperature as a function of the feed rate. Machining series 3,  $L_c = 35$  mm.

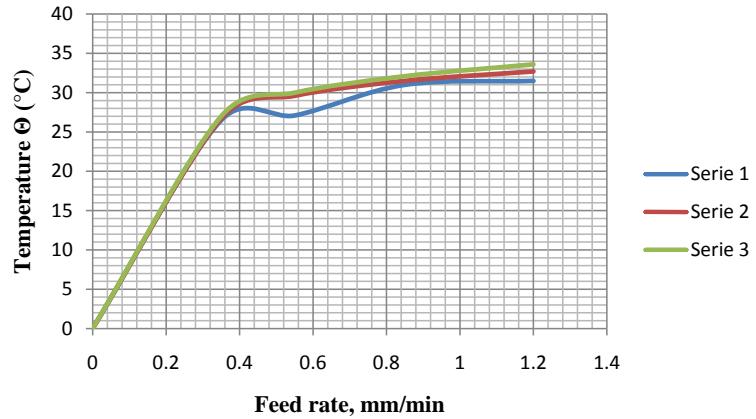


**Figure 22.** Curves of temperature as a function of the feed rate. Machining series 4,  $L_c = 25$  mm.

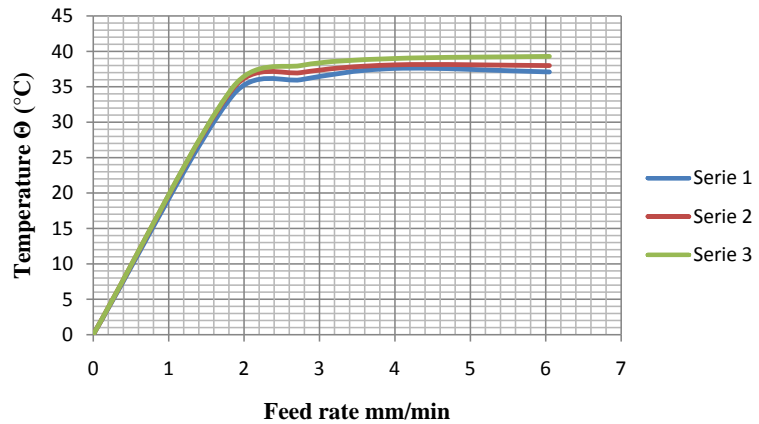


**Figure 23.** Curves of temperature as a function of the feed rate. Machining series 5,  $L_c = 25$  mm.

**For machining series 1 we find:**

- A rise in the speed of cut ranging from 0.25 to 0.35 mm/min with a ratio of 1.48 leads to the rise in temperature of the cutting tool  $\theta_{max}$  equal to 30°C;
- An increase in the speed of cut ranging from 0.55 to 0.85 mm/min with a ratio of 1.51, leads to an increase in the temperature of the cutting tool  $\theta_{max}$  equal to 33.6°C.

**For machining series 2 we find:**

- A rise in the speed of cut ranging from 1.2 to 1.85 mm/min with a ratio of 1.54 leads to the rise in temperature of the cutting tool  $\theta_{max}$  equal to 35°C;
- An increase in the speed of cut ranging from 2.75 to 4 mm/min with a ratio of 1.45, leads to an increase in the temperature of the cutting tool  $\theta_{max}$  equal to 39.9°C.

**For machining series 3 we find:**

- A rise in the speed of cut ranging from 4 to 6.05 mm/min with a ratio of 1.51 leads to the rise in temperature of the cutting tool  $\theta_{max}$  equal to 39.3°C;
- An increase in the speed of cut ranging from 9.1 to 13.3 mm/min with a ra-

tio of 1.46, leads to an increase in the temperature of the cutting tool  $\theta$  maxi equal to 42.9°C.

**For machining series 4 we find:**

- A rise in the speed of cut ranging from 0.35 to 0.55 mm/min with a ratio of 1.57 leads to the rise in temperature of the cutting tool  $\theta$  max equal to 30°C;

- An increase in the speed of cut ranging from 0.85 to 1.2 mm/min with a ratio of 1.41 leads to an increase in the temperature of the cutting tool  $\theta$  maxi equal to 33.6°C.

**For machining series 5 we find:**

- A rise in the speed of cut ranging from 1.85 to 2.75 mm/min with a ratio of 1.48 leads to the rise in temperature of the cutting tool  $\theta$  max equal to 38°C;

- An increase in the speed of cut ranging from 4 to 6.05 mm/min with a ratio of 1.51 leads to an increase in the temperature of the cutting tool  $\theta$  max equal to 39.3°C.

### 3.10. Proposed Mathematical Model

From the dimensional analysis provided above, the mathematical model proposed is given in Equation (3.1); coefficient where determined using experimental data.

$$T = \frac{\theta \cdot \lambda}{V^4 \cdot \rho} \quad (3.1)$$

where  $T$ : Effective machining time of the cutting tool in seconds ( $S$ );

$V$  Speed of cut ( $m/s$ );  $\theta$  Cutting temperature ( $^{\circ}C$ );  $\lambda$  Thermal conductivity ( $Kg \cdot m / (S^3 \cdot K)$ )

This mathematical model, which integrates the temperature parameter of the cutting tool, will make it possible to calculate the service life of the cutting tools during the machining of mechanical parts.

## 4. Conclusions

This paper addressed the problem of wear of cutting tools during machining. A reliable wear law model will provide a great tool for manufacturer when conducting their production process, and will be cost effective for their activities. This article focused on the development of the mathematical model of the service life of cutting tools (law of wear). The proposed model comes to improve the existing models of Taylor. The work presented has two parts, an experimental part and a theoretical part. Sets of machining experiments were made on a treated mild steel specimen of grade S235JR of cylindrical shape. Mild steel was chosen because it has wide application in manufacture. For each set of experiment temperature was measured using a SCT-1000 temperature sensor, and parameters such as feed rate, speed of cut and depth of pass were monitored. The experiments carried out permitted us to determine the relationship between the above listed parameters and the temperature. A new wear law has been designed using experimental data using Rayleigh-Ham dimensional analysis method.

The main findings of this study were that:

- For a high rotational speed (N in rpm) and with a low depth of cut (ap) and a medium feed rate (F in mm/min), a minimum increase in temperature at the nose of the cutting tool.

- For a minimum increase in temperature ( $\theta^{\circ}\text{C}$ ) at the cutting edge of the tool is an average rotational speed (N in rpm), with an average depth of cut (ap) and a speed d high feed rate (F in mm/min). A minimum machining time (T) is obtained.

The experimental results allowed the design of mathematical model using Rayleigh-Ham dimensional analysis method, which will permit the calculation of the machining time as a function of the cutting the temperature.

### Acknowledgements

This experimental work took place at the E3M Laboratory located in the workshops of the Ecole Nationale Supérieure Polytechnique de Douala (ENSPD) of the University of Douala with a view to writing a doctoral/Ph.D. thesis. We address our sincere thanks to the Director of the ENSPD, for having provided us with all the equipment that enabled us to carry out this work. Our thanks go to the Director and co-Director of this thesis for the advice on the choice of equipment and for monitoring this work in the laboratory.

### Conflicts of Interest

The authors declare no conflicts of interest regarding the publication of this paper.

### References

- [1] Bedrin, C. (1976) Généralités sur la coupe et l'usure des outils. Recueil de conférences: L'usure des outils dans la coupe des métaux. INSA de Lyon.
- [2] Padilla, P., Anselmetti B., Mathieu L. and Raboyeau M. (1986) Production mécanique. Fabrication générale. Bordas, Paris, 35-50.
- [3] Yang, W.H. and Tarng, Y.S. (1998) Design Optimization of Cutting Parameters for Turning Operations Based on the Taguchi Method. *Journal of Materials Processing Technology*, **84**, 122-129. [https://doi.org/10.1016/S0924-0136\(98\)00079-X](https://doi.org/10.1016/S0924-0136(98)00079-X)
- [4] Lalwani, D.I., Mehta, N.K. and Jain, P.K. (2008) Experimental Investigations of Cutting Parameters Influence on Cutting Forces and Surface Roughness in Finish Hard Turning of MDN250 Steel. *Journal of Materials Processing Technology*, **206**, 167-179. <https://doi.org/10.1016/j.jmatprotec.2007.12.018>
- [5] Ghasempoor, A., Jeswiet, J. and Moore, T.N. (1999) Real Time Implementation of On-Line Tool Condition Monitoring in Turning. *International Journal of Machine Tools and manufacture*, **39**, 1883-1902. [https://doi.org/10.1016/S0890-6955\(99\)00035-8](https://doi.org/10.1016/S0890-6955(99)00035-8)
- [6] Vergnas, J. (1982) Usinage, Technologie et Pratique. Génie Mécanique, Dunod, Paris.
- [7] Ilunga, J.C.M., Mpoyi, D.K. and Ugwiri, M.A. (2018) Contribution à l'amélioration de la surveillance de l'usure de l'outil de coupe en tournage par analyse des signaux

- vibratoires: Analyse de la puissance de coupe. *International Journal of Innovation and Applied Studies*, **24**, 602-612. <http://www.ijias.issr-journals.org/>
- [8] Krishnakumar, P., Rameshkumar, K. and Ramachandran, K. (2015) Tool Wear Condition Prediction Using Vibration Signals in High Speed Machining (HSM) of Titanium (Ti-6AL-4v) Alloy. *Procedia Computer Science*, **50**, 270-275. <https://doi.org/10.1016/j.procs.2015.04.049>
- [9] Lauro, C.H., Brandão, L.C., Baldo, D., Reis, R.A. and Davim, J.P. (2014) Monitoring and Processing Signal Applied in Machining Processes—A Review. *Measurement*, **58**, 73-86. <https://doi.org/10.1016/j.measurement.2014.08.035>
- [10] Chandra, N. (2020) Systèmes intégrés de surveillance de l'état des outils et leurs Applications: Un Examen Complet. *Procedia Manufacturing*, **48**, 852-886.
- [11] Attanasio, A., Ceretti, E., Fiorentino, A., Cappellini, C. and Giardini, C. (2010) Investigation and FEM-Based Simulation of Tool Wear in Turning Operations with Uncoated Carbide Tools. *Wear*, **269**, 344-350. <https://doi.org/10.1016/j.wear.2010.04.013>
- [12] Barlier, C. and Poulet, B. (1999) Mémothec. Génie Mécanique. 2nd Edition, Castella, Toulouse.
- [13] Attanasio, A., Gelfi, M., Giardini, C. and Remino, C. (2006) Minimal Quantity Lubrication in Turning: Effect on Tool Wear. *Wear*, **260**, 333-338. <https://doi.org/10.1016/j.wear.2005.04.024>
- [14] Trent, E.M. and Wright, P.K. (2000) Chapter 5-Heat in Metal Cutting. In: *Metal Cutting, Fourth Edition*, Butterworth-Heinemann, Oxford. <https://doi.org/10.1016/B978-075067069-2/50007-3>
- [15] Amiri, M. and Soleimani, S. (2021) ML-Based Group Data Processing Method: An Improvement over Conventional GMDH. *Complex & Intelligent Systems*, **7**, 2949-2960. <https://doi.org/10.1007/s40747-021-00480-0>
- [16] Weil, R. (1971) Techniques d'usinage. Dunod, Paris.
- [17] Geiskopf, F., CoLandon, Y. and Duc, E. (1999) Usinage à grande vitesse. Rapport ENS Cachan, LURPA.
- [18] Bouziane, A., Boulanouar, L., Azizi, M.W. and Keblouti, O. (2016) Etude de l'effet de la vitesse de coupe sur l'usure des outils de coupe en carbure métallique revêtu et non revêtu. *Proceedings of Third International Conference of Energy, Materials, Applied Energetics and Pollution (ICEMAEAP)*, Constantine, 30-31 October 2016, 1030-1035.
- [19] Bouacha, K., Yallese, M.A., Mabrouki, T. and Rigal, J.-F. (2010) Statistical Analysis of Surface Roughness and Cutting Forces Using Response Surface Methodology in Hard Turning of AISI 52100 Bearing Steel with CBN Tool. *International Journal of Refractory Metals and Hard Materials*, **28**, 349-361. <https://doi.org/10.1016/j.ijrmhm.2009.11.011>
- [20] Hessainia, Z., Yallese, M.A., Lakhdar, B. and Tarek, M. (2015) On the Application of Response Surface Methodology for Predicting and Optimizing Surface Roughness and Cutting Forces in Hard Turning by PVD Coated Insert. *International Journal of Industrial Engineering Computations*, **6**, 267-284. <https://doi.org/10.5267/j.ijiec.2014.10.003>
- [21] Baizeau, (2016) Prediction of Surface Integrity Using Flamant—Boussinesq Analytical Model. *CIRP Annals*, **65**, 81-84. <https://hal.archives-ouvertes.fr/hal-01361335> <https://doi.org/10.1016/j.cirp.2016.04.043>
- [22] Zheng, G., Xu, R., Cheng, X., Zhao, G., Lia, L. and Zhao, J. (2018) Effect of Cutting

- Parameters on Wear Behavior of Coated Tool and Surface Roughness in High-Speed Turning of 300M. *Measurement*, **125**, 99-108.  
<https://www.elsevier.com/locate/measurement>  
<https://doi.org/10.1016/j.measurement.2018.04.078>
- [23] Brocaïl, J., Watremez, M. and Dubar, L. (2010) Identification of a Friction Model for Modelling of Orthogonal Cutting. *International Journal of Machine Tools and Manufacture*, **50**, 807-814. <https://doi.org/10.1016/j.ijmachtools.2010.05.003>
- [24] Abhang, L.B. and Hameedullah, M. (2010) Chip-Tool Interface Temperature Prediction Model for Turning Process. *International Journal of Engineering, Science and Technology*, **2**, 382-393.
- [25] Duan, R., Deng, J., Ge, D., Ai, X., Liu, Y., Meng, R., Li, X. and Chen, H. (2018) A Thermo-Mechanical Coupled Model of Derivative Cutting of Microtextured Tools. *The International Journal of Advanced Manufacturing Technology*, **98**, 2849-2863.  
<https://doi.org/10.1007/s00170-018-2483-y>
- [26] Ghodam, S.D. (2014) Temperature Measurement of a Cutting Tool in Turning Process by Using Tool Work Thermocouple. *International Journal of Research in Engineering and Technology*, **3**, 831-835.  
<https://doi.org/10.15623/ijret.2014.0304147>
- [27] Kus, A., Isik, Y., Cakir, M.C., Coşkun, S. and Özdemir, K. (2015) Thermocouple and Infrared Sensor-Based Measurement of Temperature Distribution in Metal Cutting. *sensors*, **15**, Article 1274-1291. <https://www.mdpi.com/journal/sensors>  
<https://doi.org/10.3390/s150101274>
- [28] Amritkar, A., Prakash, C. and Kulkarni, A. (2012) Development of Temperature Measurement Setup for Machining. *World Journal of Science and Technology*, **2**, 15-19.
- [29] Vergnas, J. (1982) Usinage, Technologie et Pratique. Génie Mécanique, Dunod, Malakoff.
- [30] GERMAIN, D. (2011) Développement d'un modèle d'efforts de coupe intégrant le contact en dépouille: Application au tournage de super finition du cuivre Cu-c2. Ph.D. Thesis, Ecole Nationale Supérieure d'Arts et Métiers, Paris.
- [31] Kaymakci, M., Kilic, Z.M. and Altintas, Y. (2012) Unified Cutting Force Model for Turning, Boring, Drilling and Milling Operations. *International Journal of Machine Tools and Manufacture*, **54-55**, 34-45.  
<https://doi.org/10.1016/j.ijmachtools.2011.12.008>
- [32] Chinchankar, S. and Choudhury, S.K. (2016) Modélisation de la force de coupe en tenant compte de l'effet d'usure de l'outil lors du tournage en acier allié AISI 4340 durci à l'aide de multicouches Outils en carbure revêtus de TiCN/Al<sub>2</sub>O<sub>3</sub>/TiN. *The International Journal of Advanced Manufacturing Technology*, **83**, 1749-1762.  
<https://doi.org/10.1007/s00170-015-7662-5>
- [33] Orta, K. and Shoudhury, S.K. (2018) Modélisation mécaniste pour prédire les efforts de coupe lors de l'usinage en tenant compte de l'effet du rayon du nez de l'outil sur la formation de copeaux et la zone d'usure de l'outil. *International Journal of Mechanical Sciences*, **142-143**, 255-268.  
<https://doi.org/10.1016/j.ijmecsci.2018.05.004>
- [34] Babouri, M.K., Ouelaa, N. and Djeba, A. (2012) Identification de l'évolution de l'usure d'un outil de tournage basée sur l'analyse des efforts de coupe et des vibrations. *Synthèse. Revue des Sciences et de la Technologie*, **24**, 123-134.